www.amlett.com, www.vbripress.com/aml, DOI: 10.5185/amlett.2015.5927 Published online by the VBRI Press in 2015

Ion induced modification of structural and photoluminescence properties of $Y_2O_3:Eu^{3+}/Tb^{3+}$ nanophosphors: A comparative study

S. Som[1,2], S. Dutta[2], Subrata Das[1,2,*], Mukesh Kumar Pandey[3], Ritesh Kumar Dubey[4], S. P. Lochab[5], S. K. Sharma[2*]

[1]*Department of Chemical Engineering, National Taiwan University, Taipei 10617, Taiwan*
[2]*Department of Applied Physics, Indian School of Mines, Dhanbad 826004, India*
[3]*Institute of Atomic and Molecular Sciences, Academia Sinica, Taipei 10617, Taiwan*
[4]*Department of Physics, S.G.R.P.G. College, Dobhi, Purvanchal University, Jaunpur 222148, India*
[5]*Inter University Accelerator Centre, New Delhi 110067, India*

[*]Corresponding author. Tel: (+91) 3262235412; E-mail: physubrata@yahoo.co.in; sksharma.ism@gmail.com

Received: 31 March 2015, Revised: 19 April 2015 and Accepted: 21 April 2015

ABSTRACT

Herein, a comparative study on the structural and luminescence properties of optimized $Y_2O_3:Eu^{3+}/Tb^{3+}$ nanophosphor has been reported after 150 MeV Ni^{7+}, 120 MeV Ag^{9+} and 110 MeV Au^{8+} ion beam irradiation at various fluences ranging from 1×10^{11} to 1×10^{13} ions/cm^2. The X-ray diffraction results confirm the cubic phase in case of unirradiated $Y_2O_3:Eu^{3+}/Tb^{3+}$ nanophosphor. The loss of crystallinity was observed after ion irradiation and Au ion is more effective to damage the crystal structure in these phosphors. The transmission electron microscopic results show the reduction of the particle size from 100 nm to 50, 30 and 20 nm after ion irradiation with the Ni^{7+}, Ag^{9+} and Au^{8+} ions, respectively. Diffuse reflectance spectra show a blue shift in the absorption band owing to the increase in the band gap after ion irradiation. An increase in the photoluminescence intensity without any shift in the peak positions was observed with the increase in the ion fluence. The colour tunability was observed with ion irradiation as the colour coordinate varies from red to white chromaticity.

Keywords: Nanophosphor; swift heavy ion; band gap; colour tunability.

Introduction

Yttrium oxide, as one of the promising host materials for various photonic applications, is used in plasma display panels (PDPs), field emission displays (FEDs), cathode ray tubes (CRTs), fluorescent lamps, lasers and different detector devices, etc [**1-3**]**.** Identical ionic radii and similar chemical properties of Y^{3+} with other rare earth ions make Y_2O_3 as one of the best hosts for various rare earth ions. Rare earth doped Y_2O_3 has excellent luminescent properties, such as narrow emission lines and long luminescent lifetime, which are essential for potential applications in solar cells and display devices [**4-6**]**.** The rare earth emission from doped Y_2O_3 can be enhanced by codoping of another rare earth ion via the non-radiative energy transfer from one rare earth ion to another. Terbium (Tb^{3+}) and europium (Eu^{3+}) codoped compounds have been extensively studied due to their unique spectral properties including colour tunability and white light emission. Plenty of works reported the photoluminescence (PL) studies of Eu^{3+}/Tb^{3+} codoped Y_2O_3 phosphors [**7-8**]**.** But there is no detailed analysis carried out for the modification of structural and optical properties of heavy ions irradiated Eu^{3+}/Tb^{3+} codoped Y_2O_3 phosphors.

Generally, swift heavy ion (SHI) has the ability to modify the materials at molecular and electronic level by the production of defects and colour centres in the target materials [**9-12**]**.** While passing through the materials, SHI suffers a significant energy loss and high energy deposition which results into high pressure and temperature conditions in the target material [**13, 14**]**.** It enables the materials to displace from the equilibrium conditions and further help the system in achieving unique properties [**15, 16**]**.**

In our previous report, $Y_2O_3:Eu^{3+}/Tb^{3+}$ nanophosphors were prepared via combustion synthesis and the energy transfer from Tb^{3+} to Eu^{3+} was established for solid state lighting application [**7**]**.** Till date, no work has been reported on the SHI induced modification of structural and optical properties of $Y_2O_3:Eu^{3+}/Tb^{3+}$ nanophosphors. Keeping this in view, the present research work aims at the comparative investigation of structural and optical properties of virgin/ unirradiated and ion irradiated $Y_2O_3:Eu^{3+}/Tb^{3+}$ nanophosphors. The codoped phosphors with mass ratio Eu^{3+}/Tb^{3+} = 5:1 was used for ion irradiation which was best for luminescence application as per our

previous study. The phosphors were structurally characterized via XRD and TEM. Band structure and the transitions were characterized by diffuse reflectance (DR) and photoluminescence (PL) studies.

Experimental

The Eu^{3+}/Tb^{3+} codped Y_2O_3 nanophosphors were synthesized via combustion route taking Y_2O_3, Eu_2O_3, Tb_4O_7, urea and nitric acid as starting raw materials as per our previous report **[7]**. For swift heavy ion (SHI) irradiation, the 15UD pelletron of Inter University Accelerator Centre (IUAC), New Delhi, was used [**17-23**]. Details regarding the SHI irradiation for powder sample are reported elsewhere [**24-27**]. The schematic diagram of this arrangement to irradiate powder sample is shown in **Scheme 1**.

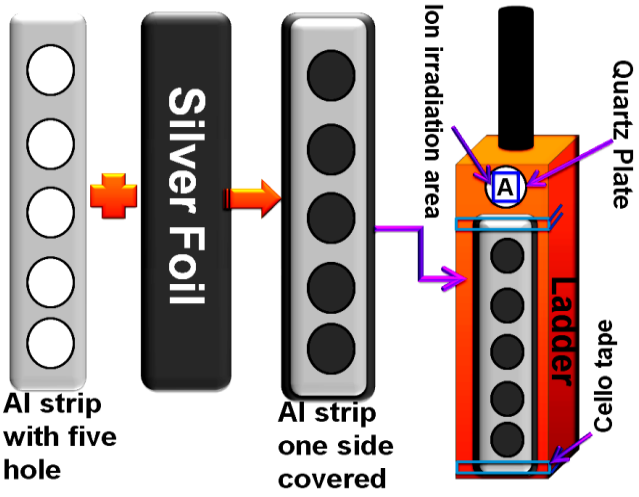

Scheme 1. SHI irradiation arrangement for powder sample.

X-ray diffractogram of virgin and ion irradiated phosphors were recorded using Bruker D8 Focus instrument with Cu target radiation (λ = 0.154056 nm). The morphology and crystallite size of the phosphors were determined by JEOL make JEM-2100 transmission electron microscope (TEM). The diffuse reflectance (DR) spectra were recorded using Perkin Elmer make Lambda 35, UV-VIS Spectrophotometer fitted with integrating sphere assembly in the wavelength range 200–800 nm. The photoluminescence (PL) studies were carried out on Hitachi Fluorescence Spectrometer F-2500.

Results and discussion

Fig. 1(a) shows the comparative XRD pattern of unirradiated and Ni, Ag and Au ion irradiated Eu^{3+}/Tb^{3+} codped Y_2O_3 nanophosphors at the ion fluence of 1×10^{13} ions/cm^2. The XRD peaks were identified and indexed according to the JCPDS file No. 83-0927 of Y_2O_3. The sharp and single diffraction peaks of unirradiated Eu^{3+}/Tb^{3+} codoped Y_2O_3 nanophosphor was the indication of single phase compounds without any impurity **[7].** No peak corresponding to the dopant elements was observed. It indicates that doping/codoping does not affect the basic crystal structure as the ionic configuration of the dopants match well with Y^{3+}.

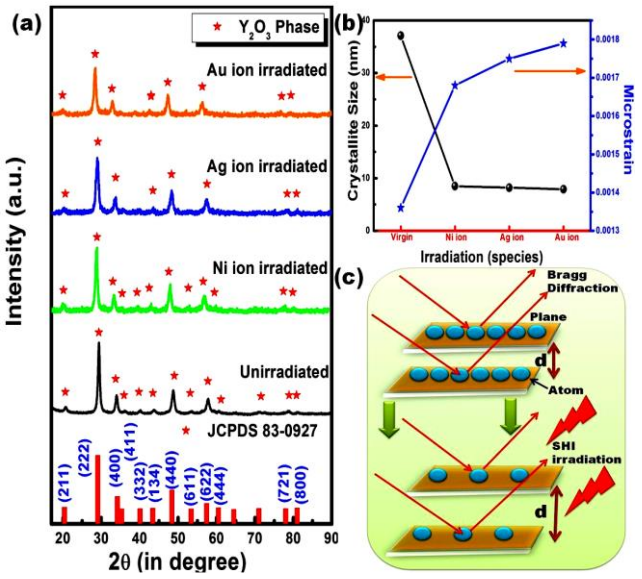

Fig. 1. (a) XRD spectra of unirradiated, Ni ion, Ag ion and Au ion irradiated Y_2O_3:Eu^{3+}/Tb^{3+} nanophosphors, (b) Crystallite size and microstrain variation of ion irradiated Y_2O_3:Eu^{3+}/Tb^{3+} nanophosphors, and (c) Schematic representation of the increase in inter-planar spacing with ion irradiation.

From literature survey, it is clear that the acceptable percentage difference (D_r) in ionic radii between the doped (R_d) and substituted ion (R_s) must not exceed 30%. In the present case D_r is calculated according to the formula $D_r = (R_s-R_d)/R_s$ and is observed as below 4% for Eu^{3+} and Tb^{3+} both [**28**]. It is the indication of the perfect replacement of Y^{3+} sites by Eu^{3+} and Tb^{3+} in this host, which is also clear from XRD results. As per JCPDS file No. 83-0927, the nanophosphor was assumed to have body centred cubic structure with space group Ia-3. The effect of swift heavy ion irradiation on this nanophosphor was also shown in **Fig. 1(a).**

The full width at half maxima (FWHM) increases and the intensity of the peak decreases owing to the irradiation. The crystallite size and microstrain of the prepared phosphors are calculated via Hall Williamson's formula for all the nanophosphors. The crystallite size is seen to be in decreasing manner and the microstrain is in increasing manner with the increase in the mass of ion species. The variation of crystallite size and microstrain with ion fluence is depicted in **Fig. 1(b)**. These structural parameters indicate the loss of crystallinity after ion irradiation [**27**]. More amorphization is observed in case of Au ion irradiated phosphors. It indicates that Au ion is more effective to this phosphor. No new peak has been observed after ion irradiation. It indicates that no new phase is obtained after ion irradiation in these phosphors. The XRD peak of the ion irradiated sample has shifted towards lower angle side. This can be explained by the Bragg's formula $2dsin\theta=n\lambda$. Here, d is inter-planar spacing, 2θ is the diffraction angle and λ is the incident wavelength. For a fixed wavelength d is inversely proportional to θ. As in the present case θ lowers indicates the increment of the inter-planar spacing after the ion irradiation [**28**]. This fact is schematically described in **Fig. 1(c).**

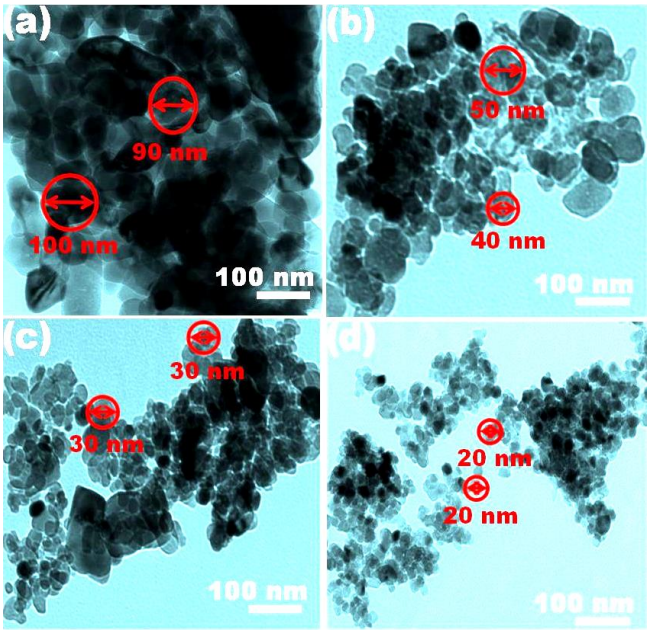

Fig. 2. TEM images of (a) unirradiated, and (b) Ni ion, (c) Ag ion and (d) Au ion irradiated Y_2O_3:Eu^{3+}/Tb^{3+} nanophosphors.

Fig. 2 shows the comparative TEM images of unirradiated and Ni, Ag and Au ion irradiated Eu^{3+}/Tb^{3+}-codoped Y_2O_3 nanophosphors at the ion fluence of 1×10^{13} ions/cm^2. **Fig. 2(a)** shows the TEM image of the unirradiated nanophosphor. The micrograph reveals a well-defined particle-like morphology with particle size ~ 100 nm, having an abundance of spherical-shaped particles with agglomeration. The change in surface morphology is observed for Ni, Ag and Au ion irradiated phosphors as shown in **Fig. 2(b-d)** respectively. Swift heavy ion breaks the agglomerated particles into irregular shaped particles with reduced particle size [**29**].

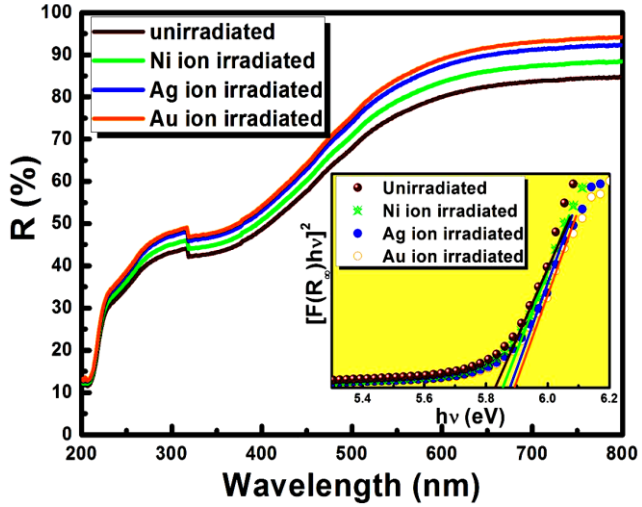

Fig. 3. Comparative DR spectra of unirradiated and Ni, Ag and Au ion irradiated Y_2O_3:Eu^{3+}/Tb^{3+} nanophosphors. Inset: Estimation of band gap for unirradiated and Ni, Ag and Au ion irradiated Y_2O_3:Eu^{3+}/Tb^{3+} nanophosphors.

Fig. 3 shows the DR spectra of Y_2O_3:Eu^{3+}/Tb^{3+} nanophosphor. It shows the sharp band at 210 nm, since the lights having this particular wavelength has been absorbed. The band at 210 nm is due to band gap of the host lattice, and no absorption band due to meta-stable energy states is found owing to the suppression of those absorption bands by *f-d* transition of Tb^{3+} occurring at 302 nm. In case of Ni, Ag and Au ion irradiated samples, the main absorption band shifts towards blue region. This shift is observed due to reduced size of crystallite with increasing ion fluence.

The band gap for Eu^{3+}/Tb^{3+} codoped Y_2O_3 nanophosphors, before and after ion irradiation, has been calculated from diffuse reflectance spectra using Kubelka Munk theory as reported elsewhere **[7],** and is shown in the inset of **Fig. 3**. The band gap is calculated to be 5.83 eV for the virgin sample. The band gap is found to increase from 5.83 eV to 5.89 eV for different ion irradiated phosphors. This is due to the decrease in the crystallite size with ion fluences. Thus swift heavy ions modify the band structure of phosphors. The tuning of band gap after swift heavy ion irradiation indicates the materials applicability in different optoelectronic devices.

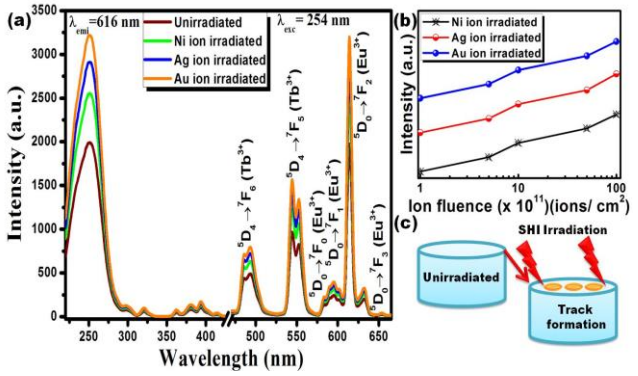

Fig. 4. (a) PL emission and excitation spectra of unirradiated and Ni, Ag and Au ion irradiated Y_2O_3:Eu^{3+}/Tb^{3+} nanophosphors. (b) The variation of PL intensity with ion fluence for different ion species. (c) Schematic representation of creation of colour centres after SHI irradiation.

Fig. 4(a) shows the excitation and emission spectra of the Y_2O_3:Eu^{3+}/Tb^{3+} nanophosphor after Ni, Ag and Au ion irradiation respectively with varying ion fluence 1×10^{11} ions/cm^2 to 1×10^{13} ions/ cm^2. The PL spectrum of the virgin sample is also added for clearer demonstration. The emission spectra are recorded at an excitation wavelength of 254 nm. The distinct emission lines, between 500–700 nm, are observed due to the $^5D_1 \rightarrow {}^7F_j$ transitions (j = 1, 2) of Eu^{3+} ions at 590 and 615 nm and sharp lines corresponding to the $^5D_4 \rightarrow {}^7F_j$ transitions of Tb^{3+} ions (j = 5, 6) at 485 and 545 nm, respectively. In the present case, the emission at 615 nm ($^5D_0 \rightarrow {}^7F_2$) is dominant suggesting that Eu^{3+} ions are located at low symmetry positions. The excitation spectra recorded at 615 nm emission contain a wide band peaking at ~250 nm, which is attributed to the CTB from O^{2-} to Eu^{3+}. In addition to the 250 nm peak, few weak peaks also appeared at 325 nm and 395 nm from the absorption of incident radiation by Eu^{3+} ions and led to the excitation of electrons from the Eu^{3+} ground state to its excited 4f levels **[7].** The DR spectra support the existence of other Eu^{3+} related weak peaks and the absence of Tb^{3+} related peaks in the excitation spectra of the codoped phosphor.

It has been observed that the luminescence emission from Au ion irradiated phosphors is greater than Ag and Ni

ion irradiated phosphors. This indicates the creation of more number of color centers and increased rate of radiative transitions after Au ion irradiation.

After ion irradiation, the peak positions remain unchanged but the intensity of peaks increases with increase of ion fluence from 1×10^{11} - 1×10^{13} ion/cm^2. The increase in PL intensity with ion fluence is shown in **Fig. 4(b)** for different ions. It can be explained on the basis of the damage and colour centres created by SHIs. Actually the greater PL intensity indicates dominant radiative transitions. The rate of radiative transition increases with the increase in the concentration of the color centers. And the grain boundaries generally act as color centers. Thus after SHI irradiation the fragmentation caused by SHIs increases, which increases the density of the grain boundaries, resulting the increase in PL emission intensity. This phenomenon is schematically explained in **Fig. 4(c).** After ion irradiation, the richness in red color and green color is observed, which this phosphor as suitable material in display devices for different color emission.

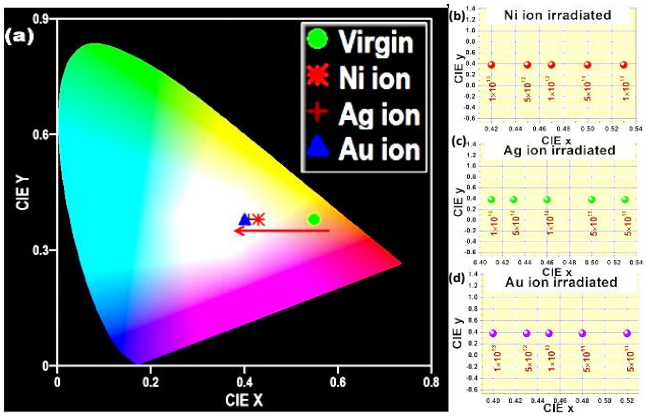

Fig. 5. (a) CIE color coordinates of Y_2O_3:Eu^{3+}/Tb^{3+} nanophosphors varying ion species. Variation of CIE coordinates with ion fluence for (b) Ni ion, (c) Ag ion, and (d) Au ion.

Fig. 5(a) shows the CIE diagram of Y_2O_3:Eu^{3+}/Tb^{3+} nanophosphor after Ni, Ag and Au ion irradiation, respectively. The CIE of the virgin sample is also added for clearer demonstration. **Fig. 5(b-d)** show the variation of colour coordinate with varying ion fluence 1×10^{11} ions/ cm^2 to 1×10^{13} ions/cm^2 for Ni, Ag and Au ion irradiation, respectively. The phosphors offer ion fluence dependent colour tuning properties indicating their applications in colour tunable solid state lighting. For ion fluence 1×10^{13} ions/cm^2 the intense colour emission is obtained for all the ions for this phosphor.

Conclusion

In this letter, the outcomes of swift heavy ion irradiations on the structural and optical properties of Y_2O_3:Eu^{3+}/Tb^{3+} nanophosphor are reported. In case of ion irradiated phosphor, the absorption band shifts towards blue region at enhanced ion fluence owing to reduced size thereby increasing the band gap. More shifts in band edge and the increased band gap has been observed for the sample irradiated with Au ions, which indicates that Au ions are more effective for modifying the band structure of Y_2O_3 phosphors compared to Ag and Ni ions. Such tuning of band gap for irradiated phosphors indicating the material's suitability in different optoelectronic devices. After ion irradiation, the luminescence intensity increases due to the increase in defect centers indicating an enhancement of radiative transitions. Au ion irradiated phosphors is found to have the maximum luminescence intensity compared to Ni and Ag ion irradiated phosphors. Richness in colour emission, colour tunability and near white light emission from ion irradiated phosphors makes Y_2O_3:Eu^{3+}/Tb^{3+} suitable for display and solid state lighting devices.

Acknowledgements

The authors are highly thankful to the Pelletron group at Inter University Accelerator Center, New Delhi, India, for providing ion beam and other facilities. The authors are also grateful to the Ministry of Science and Technology in Taiwan, ROC for financial support.

Reference

1. Ramalingam, M.; Tiwari, A. *Adv. Mat. Lett.* **2010**, *1*, 179. **DOI:** 10.5185/amlett.2010.9160
2. Zhong, J.; Liang, H.; Han, B.; Su, X.Q.; Tao, *T. Chem. Phys. Lett*., **2008**, *453*, 192. **DOI:** 10.1016/j.cplett.2008.01.032
3. Mao, Y.; Huang, J.Y.; Ostroumov, R.; Wang, K.L.; Chang, J.P. *J. Phys. Chem. C*, **2008**, *112*, 2278. **DOI:** 10.1021/jp0773738
4. Liu, X.; Li, Y.; Wang, X. *Mater. Lett*., **2006**, *60*, 1943. **DOI:** 10.1016/j.matlet.2005.12.059
5. Fukabori, A.; Sekita, M.; Ikegami, T.; Iyi, N.; Komatsu, T.; Kawamura, M.; Suzuki, M. *J. Appl. Phys*., **2007**, *101*, 043112. **DOI:** 10.1063/1.2709867
6. Huang, H.; Sun, X.; Wang, S.; Liu, Y.; Li, X.; Liu, J.; Kang, Z.; Lee, S.T. Dalton Trans., **2011**, *40*, 11362. **DOI:** 10.1039/c1dt11553g
7. Som, S.; Sharma, S. K. J. Phy. D.: *Appl. Phys*., **2012**, 45, 415102. **DOI:** 10.1088/0022-3727/45/41/415102
8. Sotiriou, G. A.; Schneider, M; Pratsinis, *S. E. J. Phys. Chem. C*, **2011**, *115(4)*, 1084. **DOI:** 10.1021/jp106137u
9. Kluth, P.; Schnohr, C.; Pakarinen, O.; Djurabekova, F.; Sprouster, D.; Giulian, R.; Toulemonde, M. *Phy.Rev. Lett.* **2008**, *101*, 175503. **DOI:** 10.1103/PhysRevLett.101.175503
10. Shukla, S.K.; Bharadvaja, A.; Tiwari, A.; Parashar, G.K.; Dubey, G.C. *Adv. Mat. Lett*. **2010**, *1(2)*, 129 **DOI:** 10.5185/amlett.2010.3105
11. Tiwari, A.; Kumar, R.; Prabaharan, M.; Pandey, R. R.; Kumari, P.; Chaturvedi, A.; Mishra, A. K. *Polym. Adv. Technol*. **2010**, *21*, 615 **DOI:** 10.1002/pat.1470
12. Ali, Y.; Kumar, V.; Sonkawade R. G.; Dhaliwal, A. S. *Adv. Mat. Lett.* **2012**, *3(5)*, 388. **DOI:** 10.5185/amlett.2012.6358
13. Szenes, G. *Phy. Rev. B*, **1999**, *60*, 3140. **DOI:** 10.1103/PhysRevB.60.3140
14. Som,S.; Dutta, S.; Chowdhury, M.; Kumar, V.; Kumar, V.; Swart, H.C.; Sharma, S.K. *J. Alloys Compds.*, **2014**, *5*, 589. **DOI:** 10.1016/j.jallcom.2013.11.182
15. Avasthi, D.K.; Mishra, Y.K.; Singh, F.; Stoquert, J.P. *Nucl. Instrum. Methods Phys. Res.*, Sect. B, **2010**, *268*, 3027. **DOI:** 10.1016/j.nimb.2010.05.033
16. Mishra, Y. K.; Chakravadhanula, V. S. K.; Schürmann, U.; Kumar, H ardeep; Kabiraj, D.; Ghosh, S.; Zaporojtchenko, V.; Avasthi, D. K; F aupel, F. *Nucl. Instrum. Methods Phys. Res., Sect. B*, **2008**, *266*, 1804. **DOI:** 10.1016/j.nimb.2008.01.040
17. Singhal, R.; Kumar, A.; Mishra., Y.K.; Mohapatra, S.; Pivin, J.C.; Avasthi, D.K.; *Nucl. Instrum. Methods Phys. Res., Sect. B*, **2008**, *266*, 3257. **DOI:** 10.1016/j.nimb.2008.04.003
18. Pivin, J.C.; Singh, F.; Mishra, Y.; Avasthi, D.K.; Stoquert, J.P. *Surf. Coat. Technol.*, **2009**, *203*, 2432. **DOI:** 10.1016/j.surfcoat.2009.02.033
19. Kaur, A.; Dhillon, A.; Lakshmi, G.B.V.S.; Mishra, Y.; Avasthi, D.K. *Mater. Chem. Phys*. **2011**, *131*, 436.

DOI: 10.1016/j.matchemphys.2011.10.001
20. Singhal, R.; Agarwal, D. C.; Mishra, Y. K.; Mohapatra, S.; Avasthi, D. K.; Chawla, A. K.; Chandra, R.; Pivin, J. C. *Nucl. Instrum. Methods Phys. Res., Sect. B*, **2009**, *267*, 1349. **DOI:** 10.1016/j.nimb.2009.01.044
21. Pal , S.; Sarkar, A.; Sanyal, D.; Rakshit, T.; Kanjilal, D.; Kumar, P.; Ray, S. K.; Jana, D. *Adv. Mater. Lett*. **2015**, *6*, 365. **DOI:** 10.5185/amlett.2015.5730
22. Kumar, V.; Sonkawade, R. G.; Dhaliwal, A. S. *Nucl. Instrum. Methods Phys. Res., Sect. B*, **2012**, *59*, 290. **DOI:** 10.1016/j.nimb.2012.08.029
23. Ali, Y.; Kumar, V.; Sonkawade, R.G.; Dhaliwal, A.S.; Swart, H.C.; *Vacuum*, **2014**, *99*, 265. **DOI:** 10.1016/j.vacuum.2013.06.016
24. Kadam, S.B.; Datta, K.; Ghosh, P.; Kadam, A.B.; Khirade, P.W.; Kumar V.; Sonkawade, R.G.; Gambhire, A.B.; Lande, M.K.; Shirsat, M.D. *Appl. Phys. A*, **2010**, *100*, 1083. **DOI:** 10.1007/s00339-010-5705-1
25. Sharma, K.; Kaith, B.S.; Kumar, V.; Kumar, V.; Kalia, S.; Kapur, B.K.; Swart, H.C. Radat. *Phys. Chem.* **2014**, *97*, 253. **DOI:** 10.1016/j.radphyschem.2013.12.008
26. Kumar, V.; Ali, Y.; Sharma, K.; Kumar, V.; Sonkawade, R.G.; Dhaliwal, A.S.; Swart, H.C. *Nucl. Instrum. Methods Phys. Res., Sect. B*, **2014**, *7*, 323. **DOI:** 10.1016/j.nimb.2014.01.009
27. Som, S.; Sharma, S. K.; Lochab, S.P. *Ceram. Int.*, **2013**, *39*, 7693. **DOI:** 10.1016/j.ceramint.2013.03.022
28. Cullity, B. D.; **1978**, *Elements of X-Ray Diffraction 2nd edn* (Reading, MA: Addison-Wesley).
29. Som, S.; Dutta, S.; Kumar, V.; Kumar, V.; Swart, H.C.; Sharma, S.K. *J. Lumin.*, **2014**, *146*, 162. **DOI:** 10.1016/j.jlumin.2013.09.058